Title: Detecting the impact of temperature on transmission of Zika, dengue and chikungunya using mechanistic models

Short title: Temperature predicts Zika, dengue, and chikungunya transmission

Authors: Erin A. Mordecai[a*], Jeremy M. Cohen[b], Michelle V. Evans[c], Prithvi Gudapati[a], Leah R. Johnson[b], Catherine A. Lippi[c], Kerri Miazgowicz[d], Courtney C. Murdock[d,e], Jason R. Rohr[b], Sadie J. Ryan[c,f,g,h], Van Savage[i,j], Marta S. Shocket[a,k], Anna Stewart Ibarra[l], Matthew B. Thomas[m], Daniel P. Weikel[n]

Affiliations:

[a]Biology Department, Stanford University, 371 Serra Mall, Stanford, CA 94305

[b]Department of Integrative Biology, University of South Florida, 4202 East Fowler Ave, SCA110 Tampa, FL 33620

[c]Department of Geography, University of Florida, PO Box 117315, Turlington Hall, Gainesville, FL 32611

[d]Center for Tropical and Emerging Global Disease, Department of Infectious Diseases, University of Georgia College of Veterinary Medicine, 501 D.W. Brooks Drive, Athens, GA 30602

[e]Odum School of Ecology, University of Georgia, 140 E. Green St., Athens, GA 30602[f]Emerging Pathogens Institute, University of Florida, P.O. Box 100009, 2055 Mowry Road Gainesville, FL 32610

[g]Center for Global Health and Translational Science, Department of Microbiology and Immunology, Weiskotten Hall, SUNY Upstate Medical University, Syracuse, NY 13210

23 [h]School of Life Sciences, College of Agriculture, Engineering, and Science, University of
24 KwaZulu Natal, Private Bag X01, Scottsville, 3209, KwaZulu Natal, South Africa
25 [i]Department of Ecology and Evolutionary Biology, University of California Los Angeles and
26 Department of Biomathematics, University of California Los Angeles, Los Angeles, CA 90095
27 [j]Santa Fe Institute, 1399 Hyde Park Rd, Santa Fe, NM 87501
28 [k]Department of Biology, Indiana University, 1001 E. 3rd St., Jordan Hall 142, Bloomington, IN
29 47405
30 [l]Center for Global Health and Translational Sciences, SUNY Upstate Medical University,
31 Syracuse, NY13210
32 [m]Department of Entomology and Center for Infectious Disease Dynamics, Penn State University,
33 112 Merkle Lab, University Park, PA 16802
34 [n]Department of Biostatistics, University of Michigan, 1415 Washington Heights, Ann Arbor, MI
35 48109

36 [*]Correspondence to: Erin Mordecai. Biology Department, Stanford University, 371 Serra Mall,
37 Stanford, CA 94305. (650) 497-7447. emordeca@stanford.edu

38 **Keywords:** Zika, dengue, chikungunya, temperature, vector transmission, *Aedes aegypti*, *Aedes*
39 *albopictus*

40

41

Abstract

Recent epidemics of Zika, dengue, and chikungunya have heightened the need to understand the seasonal and geographic range of transmission by *Aedes aegypti* and *Ae. albopictus* mosquitoes. We use mechanistic transmission models to derive predictions for how the probability and magnitude of transmission for Zika, chikungunya, and dengue change with mean temperature, and we show that these predictions are well matched by human case data. Across all three viruses, models and human case data both show that transmission occurs between 18-34°C with maximal transmission occurring in a range from 26-29°C. Controlling for population size and two socioeconomic factors, temperature-dependent transmission based on our mechanistic model is an important predictor of human transmission occurrence and incidence. Risk maps indicate that tropical and subtropical regions are suitable for extended seasonal or year-round transmission, but transmission in temperate areas is limited to at most three months per year even if vectors are present. Such brief transmission windows limit the likelihood of major epidemics following disease introduction in temperate zones.

57 **Main Text**

58 Epidemics of dengue, chikungunya, and Zika are sweeping through the Americas, and are part of
59 a global public health crisis that places an estimated 3.9 billion people in 120 countries at risk
60 (1). Dengue virus (DENV) distribution and intensity in the Americas has increased over the last
61 three decades, infecting an estimated 390 million people (96 million clinical) per year (2).
62 Chikungunya virus (CHIKV) emerged in the Americas in 2013, causing 1.8 million suspected
63 cases from 44 countries and territories (www.paho.org). In the last year, Zika virus (ZIKV) has
64 spread throughout the Americas, causing 688,040 suspected and confirmed cases, with many
65 more unreported (http://ais.paho.org/phip/viz/ed_zika_cases.asp, as of November 17, 2016). The
66 growing burden of these diseases (including links between Zika infection and both microcephaly
67 and Guillain-Barré syndrome (3)) and potential for spread into new areas creates an urgent need
68 for predictive models that can inform risk assessment and guide interventions such as mosquito
69 control, community outreach, and education.

70 Predicting transmission of DENV, CHIKV, and ZIKV requires understanding the
71 ecology of the vector species. For these viruses the main vector is *Aedes aegypti*, a mosquito that
72 prefers and is closely affiliated with humans, while *Ae. albopictus*, a peri-urban mosquito, is an
73 important secondary vector (4,5). We expect one of the main drivers of the vector ecology to be
74 the climate, particularly temperature. Along these lines, mathematical and geostatistical models
75 that incorporate climate information have been valuable for predicting and responding to *Aedes*
76 spp. spread and DENV, CHIKV, and ZIKV outbreaks (5–9).

77 The effects of temperature in ectotherms are largely predictable from fundamental
78 metabolic and ecological processes. Survival, feeding, development, and reproductive rates
79 predictably respond to temperature across a variety of ectotherms, including mosquitoes (10,11).

Because these traits help to determine transmission rates, the effects of temperature on transmission should also be broadly predictable from mechanistic models that incorporate temperature-dependent traits. Here, we introduce a model based on this framework that overcomes several major gaps that currently limit our understanding of climate suitability for transmission. Specifically, we develop models of temperature-dependent transmission for *Ae. aegypti* and *Ae. albopictus* that are (a) mechanistic, facilitating extrapolation beyond the current disease distribution, (b) parameterized with biologically accurate unimodal thermal responses for all mosquito and virus traits that drive transmission, and (c) validated against human dengue, chikungunya, and Zika case data across the Americas.

We synthesize available data to characterize the temperature-dependent traits of the mosquitoes and viruses that determine transmission intensity. With these thermal responses, we develop mechanistic temperature-dependent virus transmission models for *Ae. aegypti* and *Ae. albopictus*. We then ask whether the predicted effect of temperature on transmission is consistent with patterns of actual human cases over space and time. To do this, we validate the models with DENV, CHIKV, and ZIKV human incidence data at the country scale from the Americas from 2014-2016. To isolate temperature dependence, we also statistically controlled for population size and two socioeconomic factors that may influence transmission. If temperature fundamentally limits transmission potential, transmission should only occur at actual environmental temperatures that are predicted to be suitable, and conversely, areas with low predicted suitability should have low or zero transmission (i.e., false negative rates should be low). By contrast, low transmission may occur even when temperature suitability is high because other factors like vector control can limit transmission (i.e., the false positive rate should be higher than the false negative rate). Finally, if the simple mechanistic model accurately predicts

103 climate suitability for transmission, then we can use it to map climate-based transmission risk of
104 DENV, CHIKV, ZIKV, and other emerging pathogens transmitted by *Ae. aegypti* and *Ae.*
105 *albopictus* seasonally and geographically.

106 **Results**

107 *Temperature-dependent transmission*

108 Data gathered from the literature (9,12–14,14–20,20–29) revealed that all mosquito traits
109 relevant to transmission—biting rate, egg-to-adult survival and development rate, adult lifespan,
110 and fecundity—respond strongly to temperature and peak between 23°C and 34°C for the two
111 mosquito species (Figs. 1, S1). Humidity linearly increases survival at all mosquito life stages,
112 but does not interact with temperature (Fig. S2). DENV extrinsic incubation and vector
113 competence peak at 35°C (30–36) and 31-32°C (30,31,33,37), respectively, in both
114 mosquitoes—temperatures at which mosquito survival is low, limiting transmission potential
115 (Figs. 1, S1). Appropriate thermal response data were not available for CHIKV and ZIKV
116 extrinsic incubation and vector competence.

117

118 **Fig. 1.** Thermal responses of *Ae. aegypti* and DENV traits that drive transmission (data sources
119 listed in Table S2). Informative priors based on data from additional *Aedes* spp. and flavivirus
120 studies helped to constrain uncertainty in the model fits (see Materials and Methods; Table S3).
121 Points and error bars indicate the data means and standard errors (for display only; models were
122 fit from the raw data). Black solid lines are the mean model fits; red dashed lines are the 95%
123 credible intervals.

124

We estimated the posterior distribution of $R_0(T)$ and used it to calculate the mean and 95% credible intervals (95% CI) on the critical thermal minimum, maximum, and optimum temperature for transmission by the two mosquito species. At constant temperature, *Ae. aegypti* transmission peaked at 29.1°C (95% CI: 28.4 – 29.8°C), and declined to zero below 17.8°C (95% CI: 14.6 – 21.2°C) and above 34.6°C (95% CI: 34.1 – 35.6°C) (Fig. 2). *Ae. albopictus* transmission peaked at 26.4°C (95% CI: 25.2 – 27.4°C) and declined to zero below 16.2°C (95% CI: 13.2 – 19.9°C) and above 31.6°C (95% CI: 29.4 – 33.7°C) (Fig. 2). Overall, the thermal response curve for *Ae. albopictus* is shifted towards lower temperatures than *Ae. aegypti,* so *Ae. albopictus* transmission is better suited to colder environments. For a more realistic scenario in which daily temperature ranged over 8°C, the transmission peak, minimum, and maximum were slightly lower for both *Ae. aegypti* (28.5°C, 13.5°C, 34.2°C, respectively) and *Ae. albopictus* (26.1°C, 11.9°C, and 28.3°C, respectively). The lower thermal maximum under fluctuating temperatures occurs because we incorporated empirically supported irreversible lethal effects of temperatures that exceed thermal maxima for survival (see Materials and Methods).

Fig. 2. Relative R_0 across constant temperatures (°C; top) for *Ae. albopictus* (light blue lines and shading) and *Ae. aegypti* (dark blue lines and shading), and histograms of the posterior distributions of the critical thermal minimum (bottom left), temperature at peak transmission (bottom middle), and critical thermal maximum (bottom right; all in °C). Solid lines: mean posterior estimates; dashed lines: 95% credible intervals. R_0 curves normalized to a 0-1 scale for ease of comparison and visualization.

147 The posterior distribution of $R_0(T)$ allows us to evaluate uncertainty in key model
148 outcomes, including critical thermal minimum, maximum, and optimum. Uncertainty was higher
149 for the critical thermal minimum for transmission than for the maximum or optimum, and the
150 two mosquito species overlapped most for this outcome (Fig. 2, bottom panels). This occurred
151 because several trait thermal responses increase gradually from low to mid temperatures but
152 decline more steeply at high temperatures (Fig. 1), so uncertainty is greatest at low temperatures.
153 *Ae. aegypti* has a substantially higher optimum and maximum temperature than *Ae. albopictus*
154 (Fig. 2) due to its greater rates of adult survival at high temperatures (see Supplementary
155 Materials for sensitivity analyses).

156

157 *Model validation*

158 We used generalized linear models (GLM) to ask whether the predicted relationship
159 between temperature and transmission, $R_0(T)$, was consistent with observed human cases of
160 DENV, CHIKV, and ZIKV. Specifically, we assessed whether $R_0(T)$ was an important predictor
161 of the probability of autochthonous transmission occurring and of the incidence given that
162 transmission occurred. We also controlled for human population size, virus species, and two
163 socioeconomic factors. (Note that we focused on testing the $R_0(T)$ model, rather than on
164 constructing the best possible statistical model of human case data.) To do this, we used the
165 version of the *Ae. aegypti* $R_0(T)$ model that includes 8°C daily temperature range, along with
166 country-scale weekly case reports of DENV, CHIKV, and ZIKV in the Americas and the
167 Caribbean between 2014-2016. We first addressed the fact that countries with larger populations
168 have greater opportunities for (large) epidemics by creating two predictors that incorporate
169 scaled $R_0(T)$ and population size. In the models of the probability of autochthonous transmission

170 occurring we used the product of the posterior probability that $R_0(T) > 0$ (which we notate as
171 GR_0) and the log of population size (p) to give $log(p)*GR_0$. In the models of incidence given that
172 transmission does occur we used the log of the product of simple $R_0(T)$ and population size
173 $log(p*R_0(T))$. To control for several socioeconomic factors that might obscure the impact of
174 temperature, we also included log of gross domestic product (GDP) and log percent of GDP in
175 tourism (using logs to improve normality). These are potential indicators of investment in and/or
176 success of vector control and infrastructure improvements that prevent transmission. By
177 comparing models that included the $R_0(T)$ metric alone, socioeconomic factors alone, or both, we
178 tested whether $R_0(T)$ was an important predictor of observed transmission occurrence and
179 incidence (see Table S4). We used both in-sample and out-of-sample analyses to assess the fit of
180 each model, focusing on whether or not the $R_0(T)$ metric was included in each of the best models.

181 For the probability of autochthonous transmission occurring, the model that included both
182 the $R_0(T)$ predictor and socioeconomic predictors had overwhelming support based on Bayesian
183 Information Criterion (BIC; model PA5 relative probability = 1, Table S4). Based on deviance
184 explained, the models that included $R_0(T)$, with or without the socioeconomic predictors out-
185 performed the model that did not include $R_0(T)$ (Table S4; Figs. 3A, S3). In analyses of out-of-
186 sample accuracy, models that included the $R_0(T)$ metric (with or without the socioeconomic
187 factors) were surprisingly accurate. They predicted the probability of transmission with 86-91%
188 out-of-sample accuracy for DENV (Table S4). For CHIKV and ZIKV, models that included the
189 $R_0(T)$ metric or population alone had 66-69% out-of-sample accuracy (Table S4). There were no
190 significant differences in out-of-sample accuracy between the top four models but for both
191 DENV and CHIKV/ZIKV the best model was significantly better than the worst model (see
192 Supplementary Code for full results). The lower out-of-sample accuracy for CHIKV and ZIKV

193 likely reflects the much lower frequency of positive values and the lower total sample size of this
194 dataset. All results were similar for a set of models that separated GR_0 from population size, so
195 for simplicity we show the model predictors that combines GR_0 and population size here (see
196 Table S4 and Supplementary Code for results of other models). Together, these analyses suggest
197 that $R_0(T)$ is an important predictor of transmission occurrence, but that CHIKV and ZIKV need
198 further data to better explain the probability of transmission occurrence (Figs. 3A, S3).

199

200 **Fig. 3**. *Ae. aegypti* $R_0(T)$ and population size predict the probability and magnitude of
201 transmission of DENV, CHIKV, and ZIKV across the Americas. A, $log(p)*GR_0$ (the posterior
202 probability that $R_0(T) > 0$ times the log of population size) versus the probability of local
203 transmission in the data. B, $log(p*R_0(T))$ (log of $R_0(T)$ times the population size) versus the log
204 of incidence, given that it exceeds the threshold for local transmission. Tick-marks and points:
205 human transmission occurrence and incidence data, respectively, by country-week in the
206 Americas and Caribbean. Lines and shaded areas: mean and 95% CI from GLM fits for DENV
207 (blue) and CHIKV and ZIKV (red). For simplicity, we show the models that only include the
208 covariates $log(p)*GR_0$ or $log(p*R_0(T))$, respectively, and do not include the socioeconomic
209 covariates (models PA6 and IM4 in Table S4). For each case report data point, $log(p)*GR_0$ and
210 $log(p*R_0(T))$ were calculated at the mean temperature 10 weeks prior to the reporting week (38).

211

212 $R_0(T)$ was also an important predictor of incidence, given that autochthonous
213 transmission did occur. Within-sample, incidence was best predicted by the model that included
214 both $R_0(T)$ and the socioeconomic predictors (model IM5 in Table S4) based on BIC (relative
215 probability = 1). The models that included $R_0(T)$ out-performed those that did not based on

216 deviance explained (Table S4). In out-of-sample validation, the models that included $R_0(T)$
217 explained the magnitude of incidence based on mean absolute percentage error (85-86%
218 accuracy versus 83% accuracy for models that did not include $R_0(T)$; Table S4), but this
219 difference was not statistically significant. For illustration, we show the simpler model that only
220 contains the $R_0(T)$ predictor in the main text (Fig. 3B; model IM1 in Table S4). Notably, the
221 models that contained $R_0(T)$ predicted incidence well for all three viruses, despite the lower
222 incidence of CHIKV and ZIKV.

223 The ability of the model to explain the probability and magnitude of transmission is
224 notable given the coarse scale of the human incidence versus mean temperature data (i.e.,
225 country-scale means), the lack of CHIKV- and ZIKV-specific trait thermal response data to
226 inform the model, the nonlinear relationship between transmission and incidence, and all the
227 well-documented factors other than temperature that influence transmission. Together, these
228 analyses show simple mechanistic models parameterized with laboratory data on the two
229 mosquito species and dengue virus are consistent with observed temperature suitability for
230 transmission. Moreover, the similar responses of human incidence of ZIKV, CHIKV, and DENV
231 to temperature suggest that the thermal ecology of their shared mosquito vectors is a key
232 determinant of outbreak location, timing, and intensity.

233

234 *Mapping climate suitability for transmission*

235 The validated model can be used to predict where transmission is not excluded (posterior
236 probability that $R_0(T) > 0$, a conservative estimate of transmission risk). Considering the number
237 of months per year at which mean temperatures do not prevent transmission, large areas of
238 tropical and subtropical regions, including Puerto Rico and parts of Florida and Texas, are

239 currently suitable year-round or seasonally (Fig. 4). These regions are fundamentally at risk for
240 DENV, CHIKV, ZIKV, and other *Aedes* arbovirus transmission during a substantial part of the
241 year (Fig. 4). Indeed, DENV, CHIKV, and/or ZIKV local transmission has occurred in Texas,
242 Florida, Hawaii, and Puerto Rico (www.cdc.gov). On the other hand, many temperate regions
243 experience temperatures suitable for transmission three months or less per year (Fig. 4), and the
244 virus incubation periods in humans and mosquitoes restrict the transmission window even
245 further. Temperature thus limits the potential for the viruses to generate extensive epidemics in
246 temperate areas even where the vectors are present. Moreover, many temperate regions with
247 seasonally suitable temperatures currently lack *Ae. aegypti* and *Ae. albopictus* mosquitoes,
248 making vector transmission impossible (Fig. 4, black line). The posterior distribution of $R_0(T)$
249 also allows us to map months of risk with different degrees of uncertainty (e.g., 97.5%, 50%, and
250 2.5% posterior probability that that $R_0 > 0$), ranging from the most to least conservative (Fig.
251 S5).

252

253 **Fig. 4**. Map of predicted temperature suitability for virus transmission by *Ae. albopictus* and *Ae.*
254 *aegypti*. Color indicates the consecutive months in which temperature is permissive for
255 transmission (predicted $R_0 > 0$) for *Aedes* spp. transmission based on the minimum likely range
256 (> 97.5% posterior probability that $R_0 > 0$). Black line indicates the CDC estimated range for the
257 two *Aedes* spp. in the United States. Model suitability predictions combine temperature mean
258 and 8°C daily variation and are informed by laboratory data (Figs. 1, S1) and validated against
259 field data (Fig. 3).

260

261 **Discussion**

262 Temperature is an important driver of—and limitation on—vector transmission, so
263 accurately describing the temperature range and optimum for transmission of DENV, CHIKV,
264 and ZIKV is critical for predicting their geographic and seasonal patterns of spread. We directly
265 estimated the temperature – transmission relationship using mechanistic transmission models for
266 each mosquito species (Fig. 2). These models are built using empirical estimates of the
267 (unimodal) effects of temperature on mosquito and pathogen traits that drive transmission,
268 including survival, development, reproduction, and biting rates (Figs. 1, S1). Because these trait
269 thermal responses are unimodal across the majority of ectotherm taxa and traits, and because the
270 traits combine nonlinearly to drive transmission, the emergent relationship between temperature
271 and transmission is difficult to infer directly from field data or from individual trait responses.
272 Here, we present a model of temperature-dependent DENV, CHIKV, and ZIKV transmission
273 that advances on previous models because it is mechanistic, fitted from experimental trait data,
274 and validated against human case data at a broad geographic scale (Fig. 3). This mechanistic
275 understanding is valuable for extrapolating beyond the current spatial and temporal range of
276 transmission (Fig. 4). Of the four previous mechanistic temperature-dependent *Ae. aegypti*
277 DENV or CHIKV transmission models we were able to reproduce, our model has a similar
278 optimum but higher critical thermal maximum than two of the models (39,40), and declines
279 much more steeply at high temperatures than two other models (7,9) (Fig. S6).

280 Even though the thermal response data are imperfect—for example, CHIKV and ZIKV
281 thermal response data are missing—and the human case data are reported at a coarse spatial
282 scale, the validation analyses suggest that $R_0(T)$ is an important predictor of both the probability
283 of transmission occurring and the magnitude of incidence for DENV, CHIKV, and ZIKV. This
284 has several key implications. First, temperature-dependent transmission is pervasive enough to

285 be detected at a coarse spatial scale. Second, dynamics of the mosquito predict transmission for a
286 suite of *Ae. aegypti*-transmitted viruses, without additional virus-specific information. Third,
287 climate and socio-economic factors combine to shape variation in incidence across countries.
288 Finally, these simple predictors explain a substantial proportion of the variance in both the
289 probability and intensity of transmission.

290 Predicting arbovirus transmission at a higher spatial resolution and precision will require
291 more detailed information on factors like the exposure and susceptibility of human populations,
292 environmental variation (e.g., oviposition habitat availability, seasonal and daily temperature
293 variation), and socioeconomic factors. However, as a first step our mechanistic model provides
294 valuable insight because it makes broad predictions about suitable environmental conditions for
295 transmission, it is mechanistic and grounded in experimental trait data, it is validated against
296 human case data, and its predictions are applicable across three different viruses. Using these
297 thermal response models as a scaffold, additional drivers could be incorporated to obtain more
298 precise and specific predictions about transmission dynamics, which could in turn be used for
299 public health and vector control applications. For this purpose, all code and data used in the
300 models are available as Supplementary Files.

301 The socio-ecological conditions that enabled CHIKV, ZIKV, and DENV to become the
302 three most important emerging vector-borne diseases in the Americas make the emergence of
303 additional *Aedes*-transmitted viruses likely (potentially including Rift Valley fever, yellow fever,
304 Uganda S, or Ross River viruses). Efforts to extrapolate and to map temperature suitability (Fig.
305 4) will be critical for improving management of both ongoing and future emerging epidemics.
306 Mechanistic models like the one presented here are useful for extrapolating the potential
307 geographic range of transmission beyond the current envelope of environmental conditions in

308 which transmission occurs (e.g., under climate change and for newly invading pathogens).
309 Accurately estimating temperature-driven transmission risk in both highly suitable and marginal
310 regions is critical for predicting and responding to future outbreaks of these and other *Aedes*-
311 transmitted viruses.

312 **Materials and Methods**

313 Temperature-sensitive R_0 models

314 We constructed temperature-dependent models of transmission using a previously
315 developed R_0 framework. We modeled transmission rate as the basic reproduction rate, R_0—the
316 number of secondary infections that would originate from a single infected individual introduced
317 to a fully susceptible population. In previous work on malaria, we adapted a commonly used
318 expression for R_0 for vector transmission to include the temperature-sensitive traits that drive
319 mosquito population density (11):

320 $$R_0(T) = \left(\frac{a(T)^2\, b(T)\, c(T)\, e^{-\mu(T)/PDR(T)}\, EFD(T)\, p_{EA}(T)\, MDR(T)}{N\, r\, \mu(T)^3}\right)^{1/2} \quad (1)$$

321 Here, (T) indicates that the trait is a function of temperature, T; a is the per-mosquito biting rate,
322 b is the proportion of infectious bites that infect susceptible humans, c is the proportion of bites
323 on infected humans that infect previously uninfected mosquitoes (i.e., $b*c$ = vector competence),
324 μ is the adult mosquito mortality rate (lifespan, $lf = 1/\mu$), PDR is the parasite development rate
325 (i.e., the inverse of the extrinsic incubation period, the time required between a mosquito biting
326 an infected host and becoming infectious), EFD is the number of eggs produced per female
327 mosquito per day, p_{EA} is the mosquito egg-to-adult survival probability, MDR is the mosquito
328 immature development rate (i.e., the inverse of the egg-to-adult development time), N is the
329 density of humans, and r is the human recovery rate. For each temperature-sensitive trait in each

330 mosquito species, we fit either symmetric (Quadratic, $-c(T - T_0)(T - T_m)$) or asymmetric (Brière,
331 $cT(T - T_0)(T_m - T)^{1/2}$) unimodal thermal response models to the available empirical data (41). In
332 both functions, T_0 and T_m are respectively the minimum and maximum temperature for
333 transmission, and c is a positive rate constant.

334 We consider a relativized version of the R_0 equation because absolute values of R_0
335 depend on additional factors not captured in our model. Therefore, $R_0 > 0$ is an absolute
336 threshold for whether or not transmission is possible, but the model does not predict when
337 transmission is stable (i.e., absolute $R_0 > 1$). While absolute estimates of R_0 are difficult to obtain
338 and different model formulations can produce different results, our use of relative R_0 adequately
339 describes the nonlinear relationship between mosquito and virus traits and transmission.
340 Different expressions for R_0, including the square of equation (1), map monotonically onto our
341 function, so they produce identical estimates for the points at which transmission declines to zero
342 and peaks.

343 We fit the trait thermal responses in equation (1) based on an exhaustive search of
344 published laboratory studies that fulfilled the criterion of measuring a trait at three or more
345 constant temperatures, ideally capturing both the rise and the fall of each unimodal curve (Tables
346 S1-S2). Constant-temperature laboratory conditions are required to isolate the direct effect of
347 temperature from confounding factors in the field and to provide a baseline for estimating the
348 effects of temperature variation through rate summation (42). We attempted to obtain raw data
349 from each study, but if they were not available we collected data by hand from tables or digitized
350 data from figures using WebPlotDigitizer (43). We obtained raw data from Delatte (18) and Alto
351 (20) for the *Ae. albopictus* egg-to-adult survival probability (*pEA*), mosquito development rate
352 (MDR), gonotrophic cycle duration (GCD, which we assumed was equal to the inverse of the

353 biting rate) and total fecundity (TFD) (Table S2). Data did not meet the inclusion criterion for
354 CHIKV or ZIKV vector competence (*b, c*) or extrinsic incubation period (*EIP*) in either *Ae.*
355 *albopictus* or *Ae. aegypti*. Instead, we used DENV EIP and vector competence data, combined
356 with sensitivity analyses.

357 Following Johnson *et al.* (44), we fit a thermal response for each trait using Bayesian
358 models. We first fit Bayesian models for each trait thermal response using uninformative priors
359 (T_0 ~ Uniform (0, 24), T_m ~ Uniform (25, 45), c ~ Gamma (1, 10) for Brière and c ~ Gamma (1,
360 1) for Quadratic fits) chosen to restrict each parameter to its biologically realistic range (i.e., T_0 <
361 T_m and we assumed that temperatures below 0°C and above 45°C were lethal). Any negative
362 values for all thermal response functions were truncated at zero, and thermal responses for
363 probabilities (p_{EA}, b, and c) were also truncated at one. We modeled the observed data as arising
364 from a normal distribution with the mean predicted by the thermal response function calculated
365 at the observed temperature, and the precision τ, ($\tau = 1/\sigma$), distributed as τ ~ Gamma (0.0001,
366 00001). We fit the models using Markov Chain Monte Carlo (MCMC) sampling in JAGS, using
367 the R (45) package *rjags* (46). For each thermal response, we ran five MCMC chains with a
368 5000-step burn-in and saved the subsequent 5000 steps. We thinned the posterior samples by
369 saving every fifth sample and used the samples to calculate R_0 from 15-40°C, producing a
370 posterior distribution of R_0 versus temperature. We summarized the relationship between
371 temperature and each trait or overall R_0 by calculating the mean and 95% highest posterior
372 density interval (HPD interval; a type of credible interval that includes the smallest continuous
373 range containing 95% of the probability, as implemented in the *coda* package (47)) for each
374 curve across temperatures.

375 We fit a second set of models for each mosquito species that used informative priors to
376 reduce uncertainty in R_0 versus temperature and in the trait thermal responses. In these models,
377 we used Gamma-distributed priors for each parameter T_0, T_m, c, and τ fit from an additional
378 'prior' dataset of *Aedes* spp. trait data that did not meet the inclusion criteria for the primary
379 dataset (Table S3). We found that these initial informative priors could have an overly strong
380 influence on the posteriors, in some cases drawing the posterior distributions well away from the
381 primary dataset, which was better controlled and met the inclusion criteria. We accounted for our
382 lower confidence in this data set by increasing the variance in the informative priors, by
383 multiplying all hyperparameters (i.e., the parameters of the Gamma distributions of priors for T_0,
384 T_m, and c) by a constant k to produce a distribution with the same mean but $1/k$ times larger
385 variance. We chose the value of k based on our relative confidence in the prior versus main data.
386 Thus we chose $k = 0.5$ for b, c, and PDR and $k = 0.01$ for lf. This is the main model presented in
387 the text (Fig. 2). It is comparable to some but not all previous mechanistic models for *Ae. aegypti*
388 and *Ae. albopictus* transmission (Fig. S6). Results of our main model, fit with informative priors,
389 did not vary substantially from the model fit with uninformative priors (Figs. S7-S8).

390 Effects of humidity on dengue R_0

391 Like temperature, humidity is expected to affect vector transmission via its effects on
392 mosquito populations. Specifically, we expected humidity to affect egg-to-adult survival and
393 adult survival. Using the methods described above, we extracted experimental laboratory data on
394 these traits measured at a range of constant humidities in the laboratory. We searched for *Aedes*
395 spp. survival probability data across temperature and humidity. We obtained data on *Aedes*
396 *aegypti* egg hatching probability (48) and *Anopheles gambiae* lifespan (49), which we used in
397 absence of *Aedes* spp. because they have a similar (tropical, anthrophilic) life history. We used

398 linear regression to estimate the relationship between these traits and relative humidity (%),
399 plugged them into the $R_0(T)$ equation (assuming the probability of egg hatching and egg-to-adult
400 survival have the same relationship with humidity), and plotted R_0 versus temperature across a
401 range of relative humidity values (Fig. S2). For the dataset that included variation in temperature
402 and humidity independently, there was no interaction between the unimodal temperature
403 response and the linear humidity response (i.e., humidity did not affect the relationship between
404 lifespan and temperature) (49). The resulting relationship between R_0 and relative humidity was
405 exponential. Humidity is not included in the main models presented in the text.

406 Incorporating daily temperature variation in transmission models

407 Because organisms do not typically experience constant temperature environments in
408 nature, we incorporated the effects of temperature variation on transmission by calculating a
409 daily average R_0 assuming a daily temperature range of 8°C, across a range of mean
410 temperatures. This range is consistent with daily temperature variation in tropical and subtropical
411 environments but lower than in most temperate environments. At each mean temperature, we
412 used a Parton-Logan model to generate hourly temperatures and calculate each temperature-
413 sensitive trait on an hourly basis (50). We assumed an irreversible high-temperature threshold
414 above which mosquitoes die and transmission is impossible (51,52). We set this threshold based
415 on hourly temperatures exceeding the critical thermal maximum (T_m in Tables S1-S2) for egg-to-
416 adult survival or adult longevity by any amount for five hours or by 3°C for one hour. We
417 averaged each trait over 24 hours to obtain a daily average trait value, which we used to calculate
418 relative R_0 across a range of mean temperatures. We used this model in the validation against
419 human cases (Fig. 3) and the risk map (Fig. 4).

420 Model validation with DENV, CHIKV, and ZIKV incidence data

421 To validate the model, we used data on human cases of DENV, CHIKV, and ZIKV at the
422 country scale and mean temperature during the transmission window. Using statistical models
423 (as described below), we estimated the effects of predicted $R_0(T)$ on the probability of local
424 transmission and the magnitude of incidence, controlling for population size and several
425 socioeconomic factors. We downloaded and manually entered Pan American Health
426 Organization (PAHO) weekly case reports for DENV and CHIKV for all countries in the
427 Americas (North, Central, and South America and the Caribbean Islands) from week 1 of 2014
428 to week 8 of 2015 for CHIKV and from week 52 of 2013 to week 47 of 2015 for DENV
429 (www.paho.org). ZIKV weekly case reports for reporting districts (e.g., provinces) within
430 Colombia, Mexico, El Salvador, and the US Virgin Islands were available from the CDC
431 Epidemic Prediction Initiative (https://github.com/cdcepi/) from November 28, 2015 to April 2,
432 2016. We aggregated the ZIKV data into country-level weekly case reports to match the spatial
433 resolution of the DENV, CHIKV, and covariate data.

434

435 Temperature data collection

436 We matched the DENV, CHIKV, and ZIKV incidence data with temperature using daily
437 temperature data from METAR stations in each country, averaged at the country level by
438 epidemic week. A previous study found a six-week lagged relationship between temperature and
439 oviposition for *Aedes aegypti* in Ecuador (38). Assuming that the subsequent transmission,
440 disease development, medical care-seeking, and case reporting in humans takes an additional
441 four weeks, we assumed *a priori* a ten-week lag between temperature and incidence (i.e., mean
442 temperature for the week that is ten weeks prior to each case report). METAR stations are
443 internationally standardized weather reporting stations that report hourly temperature and

444 precipitation measures. Outlier weather stations were excluded if they reported a daily maximum
445 temperature below 5°C or a daily minimum temperature above 40°C during the study period,
446 extremes that would certainly eliminate the potential for transmission in a local area. Because
447 case data are reported at the country level, we needed a collection of weather stations in each
448 country that accurately represent weather conditions in the areas where transmission occurs,
449 excluding extreme areas where transmission is unlikely. For the study period of October 1, 2013
450 through April 30, 2016, we downloaded daily temperature data for each station from Weather
451 Underground using the *weatherData* package in R (53). We removed all data from Chile because
452 it spans so much latitude and the terrain is so diverse that its country-level mean is unlikely to be
453 very representative of the temperature where an outbreak occurred.

454 Socioeconomic covariate data

455 We accessed available data on projected 2016 gross domestic product (GDP) for
456 countries of interest via the International Monetary Fund's World Economic Outlook Database
457 (http://www.imf.org/external/ns/cs.aspx?id=28). The direct and total contributions of tourism to
458 GDP in 2016 were compiled from World Travel and Tourism Council economic impact reports
459 (http://www.wttc.org/research/economic-research/economic-impact-analysis/country-
460 reports/#undefined). We retrieved population size data for 2013-2015 from the United Nations
461 Population Division (https://esa.un.org/unpd/wpp/Download/Standard/Population/) and averaged
462 them across the three years for each country.

463 Validation analyses with human incidence versus temperature datasets

464 To validate the $R_0(T)$ model while controlling for population and socio-economic factors,
465 we used generalized linear regression on the weekly case count data. Importantly, we focused on
466 testing whether the case counts were consistent with the transmission – temperature relationship

467 predicted from our model, rather than on maximizing the variation explained in the statistical
468 model. We are more specifically interested in understanding autochthonous transmission (i.e.,
469 locally acquired, not just imported cases). We set country-level thresholds for the number of
470 cases defining autochthonous transmission for our three diseases separately, based on current
471 transmission understanding: seven cases of CHIKV, 70 cases of DENV, and three cases of
472 ZIKV. The resulting data consisted of zeros for no transmission and positive case counts when
473 transmission is presumed to be occurring. To model these data, we used a hurdle model that first
474 uses logistic regression on the presence/absence of local transmission data to understand the
475 factors correlated with local transmission occurring or not (PA analysis). Then we modeled the
476 log of incidence (number of new cases per reporting week) for positive values with a gamma
477 generalized linear models (GLM; i.e., incidence analysis).

478 We were interested in understanding whether $R_0(T)$ was an important predictor of human
479 transmission occurrence and incidence, after controlling for potentially confounding factors like
480 population size and socioeconomic conditions. To do this, we fit a series of models with different
481 subsets of predictors that included $R_0(T)$, the socioeconomic variables with population, or both
482 (see Table S4 for full models). To control for human population size, we created new metrics
483 based on $R_0(T)$ and population size to use for validation against the PAHO incidence data. We
484 define GR_0, which is the posterior probability that $R_0(T) > 0$. We use $log(p)*GR_0$, where p is the
485 population size, as the relevant R_0-based predictor for the PA analysis. For the incidence
486 analysis, we instead use $log(p*R_0(T))$ as the predictor. In all cases log refers to the natural
487 logarithm. For simplicity, we refer to these as the $R_0(T)$ metrics hereafter and in the Results.

488 In both the PA and incidence analyses, we first used the full data sets to examine which
489 of the candidate models best described the data. Randomized quantile residuals indicated that the

490 logistic and gamma GLM models were performing adequately. We compared the approximate
491 model probabilities, calculated from the BIC scores, as well as the proportion of deviance
492 explained (D^2) from each model. Next we examined the performance of the models in predicting
493 out of sample, for both PA and incidence analyses. To do this we created 1000 random
494 partitions, where 90% of the data were used to train the model and 10% were used for testing. In
495 the PA analyses we classified each partition based on presence/absence, with separate
496 classification thresholds for DENV versus CHIKV/ZIKV as these grouping had much different
497 probabilities of occurrence. We assessed the performance of the model for the PA analysis based
498 on the mean misclassification rate. In the incidence analyses we assessed the model performance
499 based on the predictive mean absolute percentage error (MAPE). Since differences in prediction
500 success between the models in both the PA and incidence analyses were not statistically
501 significant, we present the simpler models that only include the $R_0(T)$ metrics in the main text
502 (Fig. 3) and the models that additionally include socioeconomic covariates in the Supplementary
503 Information (Figs. S3-S4). We plotted the model predictions as a function of the $R_0(T)$ metrics
504 together with the observed data for the PA and incidence analyses using the R package *visreg*
505 (54).

506 Mapping temperature suitability for transmission

507 Using our validated model, we were interested in where the temperature was suitable for
508 *Ae. aegypti* and/or *Ae. albopictus* transmission for some or all of the year to predict the potential
509 geographic range of outbreaks in the Americas. We visualized the minimum, median, and
510 maximum extent of transmission based on probability of occurrence thresholds from the R_0
511 models for both mosquitoes. We calculated the number of consecutive months in which the
512 posterior probability of $R_0 > 0$ exceeds a threshold of 0.025, 0.5, or 0.975 for both mosquito

513 species, representing the maximum, median, and minimum likely ranges, respectively. The
514 minimum range is shown in Fig. 4 and all three ranges are overlaid in Fig. S5. This analysis
515 indicates the predicted seasonality of temperature suitability for transmission geographically, but
516 does not indicate its magnitude. To generate the maps, we cropped monthly mean temperature
517 rasters from 1950-2000 for all twelve months (Worldclim; www.worldclim.org/) to the Americas
518 (*R*, *raster* package, *crop* function) and assigned cells values of 1 or 0 depending on whether the
519 probability that $R_0 > 0$ exceeded the threshold at the temperatures in those cells (Table S3). We
520 then synthesized the monthly grids into a single raster that reflected the maximum number of
521 consecutive months where cell values equaled 1. The resulting rasters were plotted in ArcGIS
522 10.3, overlaying the three cutoffs (Figure 3). We repeated this process for both mosquito species.

523

524

525 **Acknowledgments**

526 Barry Alto, Krijn Paaijmans, Francis Ezeakacha, and Helene Delatte kindly provided raw data
527 used in the analyses. We gratefully acknowledge the Centers for Disease Control and Prevention
528 Epidemic Predictions Initiative (CDC EPI) for collating and sharing the Zika incidence data on
529 GitHub (https://zenodo.org/record/48946#.Vz-EM2bb8ys). The authors declare no competing
530 interests.

531

532 **Author contributions:**

533 EAM, MBT, VS, SJR, LRJ, ASI, and JRR designed the research. JMC, MVE, PG, CAL, KM,
534 CCM, MSS, DPW, and EAM conducted the research. EAM wrote the first draft of the paper and
535 all authors contributed to revisions.

References:

1. Brady OJ, Gething PW, Bhatt S, Messina JP, Brownstein JS, Hoen AG, et al. Refining the global spatial limits of dengue virus transmission by evidence-based consensus. PLOS Negl Trop Dis. 2012 Aug 7;6(8):e1760.

2. Bhatt S, Gething PW, Brady OJ, Messina JP, Farlow AW, Moyes CL, et al. The global distribution and burden of dengue. Nature. 2013 Apr 25;496(7446):504–7.

3. Rasmussen SA, Jamieson DJ, Honein MA, Petersen LR. Zika virus and birth defects — reviewing the evidence for causality. N Engl J Med. 2016 Apr 13;374:1981–7.

4. Scott TW, Takken W. Feeding strategies of anthropophilic mosquitoes result in increased risk of pathogen transmission. Trends Parasitol. 2012 Mar;28(3):114–21.

5. Messina JP, Kraemer MU, Brady OJ, Pigott DM, Shearer FM, Weiss DJ, et al. Mapping global environmental suitability for Zika virus. eLife. 2016 Apr 19;5:e15272.

6. Magori K, Legros M, Puente ME, Focks DA, Scott TW, Lloyd AL, et al. Skeeter Buster: A stochastic, spatially explicit modeling tool for studying Aedes aegypti population replacement and population suppression strategies. PLOS Negl Trop Dis. 2009 Sep 1;3(9):e508.

7. Johansson MA, Powers AM, Pesik N, Cohen NJ, Staples JE. Nowcasting the spread of chikungunya virus in the Americas. PLoS ONE. 2014 Aug 11;9(8):e104915.

8. Perkins TA, Metcalf CJE, Grenfell BT, Tatem AJ. Estimating drivers of autochthonous transmission of chikungunya virus in its invasion of the Americas. PLoS Curr [Internet]. 2015 Feb 10 [cited 2015 Aug 18];7. Available from: http://www.ncbi.nlm.nih.gov/pmc/articles/PMC4339250/

9. Morin CW, Monaghan AJ, Hayden MH, Barrera R, Ernst K. Meteorologically driven simulations of dengue epidemics in San Juan, PR. PLoS Negl Trop Dis. 2015 Aug 14;9(8):e0004002.

10. Dell AI, Pawar S, Savage VM. Systematic variation in the temperature dependence of physiological and ecological traits. Proc Natl Acad Sci. 2011 May 23;108(26):10591–6.

11. Mordecai EA, Paaijmans KP, Johnson LR, Balzer CH, Ben-Horin T, de Moor E, et al. Optimal temperature for malaria transmission is dramatically lower than previously predicted. Ecol Lett. 2013;16:22–30.

12. Focks DA, Haile DG, Daniels E, Mount GA. Dynamic life table model for Aedes aegypti (Diptera: Culicidae): analysis of the literature and model development. J Med Entomol. 1993 Nov;30(6):1003–17.

13. Yang HM, Macoris MLG, Galvani KC, Andrighetti MTM, Wanderley DMV. Assessing the effects of temperature on the population of Aedes aegypti, the vector of dengue. Epidemiol Infect. 2009;137(08):1188–202.

14. Rueda L, Patel K, Axtell R, Stinner R. Temperature-dependent development and survival rates of Culex quinquefasciatus and Aedes aegypti (Diptera: Culicidae). J Med Entomol. 1990;27(5):892–8.

15. Tun-Lin W, Burkot TR, Kay BH. Effects of temperature and larval diet on development rates and survival of the dengue vector Aedes aegypti in north Queensland, Australia. Med Vet Entomol. 2000 Mar 1;14(1):31–7.

16. Kamimura K, Matsuse IT, Takahashi H, Komukai J, Fukuda T, Suzuki K, et al. Effect of temperature on the development of Aedes aegypti and Aedes albopictus. Med Entomol Zool. 2002;53(1):53–8.

572 17. Eisen L, Monaghan AJ, Lozano-Fuentes S, Steinhoff DF, Hayden MH, Bieringer PE. The impact of
573 temperature on the bionomics of Aedes (Stegomyia) aegypti, with special reference to the cool geographic
574 range margins. J Med Entomol. 2014 May 1;51(3):496–516.

575 18. Delatte H, Gimonneau G, Triboire A, Fontenille D. Influence of temperature on immature development,
576 survival, longevity, fecundity, and gonotrophic cycles of Aedes albopictus, vector of chikungunya and dengue
577 in the Indian Ocean. J Med Entomol. 2009 Jan 1;46(1):33–41.

578 19. Muturi EJ, Lampman R, Costanzo K, Alto BW. Effect of temperature and insecticide stress on life-history traits
579 of Culex restuans and Aedes albopictus (Diptera: Culicidae). J Med Entomol. 2011 Mar;48(2):243–50.

580 20. Alto BW, Juliano SA. Temperature effects on the dynamics of Aedes albopictus (Diptera: Culicidae)
581 populations in the laboratory. J Med Entomol. 2001 Jul;38(4):548–56.

582 21. Westbrook CJ, Reiskind MH, Pesko KN, Greene KE, Lounibos LP. Larval environmental temperature and the
583 susceptibility of Aedes albopictus Skuse (Diptera: Culicidae) to chikungunya virus. Vector-Borne Zoonotic
584 Dis. 2010 Apr 28;10(3):241–7.

585 22. Briegel H, Timmermann SE. Aedes albopictus (Diptera: Culicidae): Physiological aspects of development and
586 reproduction. J Med Entomol. 2001 Jul 1;38(4):566–71.

587 23. Calado DC, Navarro-Silva MA. Influência da temperatura sobre a longevidade, fecundidade e atividade
588 hematofágica de Aedes (Stegomyia) albopictus Skuse, 1894 (Diptera, Culicidae) sob condições de laboratório.
589 Rev Bras Entomol. 2002;46(1):93–8.

590 24. Beserra EB, Fernandes CRM, Silva SA de O, Silva LA da, Santos JW dos. Efeitos da temperatura no ciclo de
591 vida, exigências térmicas e estimativas do número de gerações anuais de Aedes aegypti (Diptera, Culicidae).
592 Iheringia Sér Zool [Internet]. 2009 [cited 2015 Sep 10]; Available from: http://agris.fao.org/agris-
593 search/search.do?recordID=XS2010500501

594 25. Westbrook CJ. Larval ecology and adult vector competence of invasive mosquitoes Aedes albopictus and
595 Aedes aegypti for Chikungunya virus [Internet]. University of Florida; 2010 [cited 2013 Oct 23]. Available
596 from: http://etd.fcla.edu/UF/UFE0041830/westbrook_c.pdf

597 26. Couret J, Dotson E, Benedict MQ. Temperature, Larval Diet, and Density Effects on Development Rate and
598 Survival of Aedes aegypti (Diptera: Culicidae). PLoS ONE. 2014 Feb 3;9(2):e87468.

599 27. Ezeakacha N. Environmental impacts and carry-over effects in complex life cycles: the role of different life
600 history stages. Dissertation [Internet]. 2015 Dec 11; Available from: http://aquila.usm.edu/dissertations/190

601 28. Teng H-J, Apperson CS. Development and Survival of Immature Aedes albopictus and Aedes triseriatus
602 (Diptera: Culicidae) in the Laboratory: Effects of Density, Food, and Competition on Response to
603 Temperature. J Med Entomol. 2000 Jan 1;37(1):40–52.

604 29. Wiwatanaratanabutr S, Kittayapong P. Effects of temephos and temperature on Wolbachia load and life history
605 traits of Aedes albopictus. Med Vet Entomol. 2006;20(3):300–307.

606 30. Xiao F-Z, Zhang Y, Deng Y-Q, He S, Xie H-G, Zhou X-N, et al. The effect of temperature on the extrinsic
607 incubation period and infection rate of dengue virus serotype 2 infection in Aedes albopictus. Arch Virol.
608 2014 Jul 3;159(11):3053–7.

609 31. Watts DM, Burke DS, Harrison BA, Whitmire RE, Nisalak A. Effect of temperature on the vector efficiency of
610 Aedes aegypti for dengue 2 virus. Am J Trop Med Hyg. 1987 Jan;36(1):143–52.

32. McLean DM, Clarke AM, Coleman JC, Montalbetti CA, Skidmore AG, Walters TE, et al. Vector capability of Aedes aegypti mosquitoes for California encephalitis and dengue viruses at various temperatures. Can J Microbiol. 1974 Feb 1;20(2):255–62.

33. Carrington LB, Armijos MV, Lambrechts L, Scott TW. Fluctuations at a low mean temperature accelerate dengue virus transmission by Aedes aegypti. PLoS Negl Trop Dis. 2013 Apr 25;7(4):e2190.

34. Davis NC. The effect of various temperatures in modifying the extrinsic incubation period of the yellow fever virus in Aedes aegypti. Am J Epidemiol. 1932 Jul 1;16(1):163–76.

35. McLean DM, Miller MA, Grass PN. Dengue virus transmission by mosquitoes incubated at low temperatures. Mosq News [Internet]. 1975 [cited 2015 Aug 26]; Available from: http://agris.fao.org/agris-search/search.do?recordID=US19760088008

36. Focks DA, Daniels E, Haile DG, Keesling JE. A simulation model of the epidemiology of urban dengue fever: literature analysis, model development, preliminary validation, and samples of simulation results. Am J Trop Med Hyg. 1995 Nov;53(5):489–506.

37. Alto BW, Bettinardi D. Temperature and dengue virus infection in mosquitoes: independent effects on the immature and adult stages. Am J Trop Med Hyg. 2013 Mar;88(3):497–505.

38. Stewart Ibarra AM, Ryan SJ, Beltrán E, Mejía R, Silva M, Muñoz Á. Dengue vector dynamics (Aedes aegypti) influenced by climate and social factors in Ecuador: implications for targeted control. PLoS ONE. 2013 Nov 12;8(11):e78263.

39. Wesolowski A, Qureshi T, Boni MF, Sundsøy PR, Johansson MA, Rasheed SB, et al. Impact of human mobility on the emergence of dengue epidemics in Pakistan. Proc Natl Acad Sci. 2015 Sep 8;201504964.

40. Liu-Helmersson J, Stenlund H, Wilder-Smith A, Rocklöv J. Vectorial Capacity of Aedes aegypti: Effects of Temperature and Implications for Global Dengue Epidemic Potential. PLoS ONE. 2014 Mar 6;9(3):e89783.

41. Briere J-F, Pracros P, Le Roux A-Y, Pierre J-S. A novel rate model of temperature-dependent development for arthropods. Environ Entomol. 1999 Feb 1;28(1):22–9.

42. Lambrechts L, Paaijmans KP, Fansiri T, Carrington LB, Kramer LD, Thomas MB, et al. Impact of daily temperature fluctuations on dengue virus transmission by Aedes aegypti. Proc Natl Acad Sci. 2011 May 3;108(18):7460–5.

43. Rohatgi A. WebPlotDigitizer [Internet]. 2015. Available from: http://arohatgi.info/WebPlotDigitizer

44. Johnson LR, Ben-Horin T, Lafferty KD, McNally A, Mordecai E, Paaijmans KP, et al. Understanding uncertainty in temperature effects on vector-borne disease: a Bayesian approach. Ecology. 2015 Jan 1;96(1):203–13.

45. R Development Core Team. R: A Language and Environment for Statistical Computing [Internet]. Vienna, Austria: R Foundation for Statistical Computing; 2014. Available from: http://www.R-project.org

46. Plummer M. rjags: Bayesian Graphical Models using MCMC [Internet]. 2016. Available from: http://CRAN.R-project.org/package=rjags

47. Plummer M, Best N, Cowles K, Vines K. CODA: Convergence Diagnosis and Output Analysis for MCMC. 2006. (R News).

48. Dickerson CZ. The effects of temperature and humidity on the eggs of Aedes aegypti (L.) and Aedes albopictus (skuse) in Texas [Doctoral]. [College Station, Texas]: Texas A & M University; 2007.

49. Bayoh MN. Studies on the development and survival of anopheles gambiae sensu stricto at various temperatures and relative humidities [Internet] [Doctoral]. Durham University; 2001 [cited 2014 Oct 15]. Available from: http://etheses.dur.ac.uk/4952/

50. Parton WJ, Logan JA. A model for diurnal variation in soil and air temperature. Agric Meteorol. 1981 Jan 1;23:205–16.

51. Paaijmans KP, Heinig RL, Seliga RA, Blanford JI, Blanford S, Murdock CC, et al. Temperature variation makes ectotherms more sensitive to climate change. Glob Change Biol. 2013 Aug 1;19(8):2373–80.

52. Vasseur DA, DeLong JP, Gilbert B, Greig HS, Harley CDG, McCann KS, et al. Increased temperature variation poses a greater risk to species than climate warming. Proc R Soc Lond B Biol Sci. 2014 Mar 22;281(1779):20132612.

53. Narasimhan R. weatherData: Get Weather Data from the Web [Internet]. 2014 [cited 2016 May 25]. Available from: https://cran.r-project.org/web/packages/weatherData/index.html

54. Breheny P, Burchett W. visreg: Visualization of Regression Models [Internet]. 2016 [cited 2016 Jun 8]. Available from: https://cran.r-project.org/web/packages/visreg/index.html

Figure 1

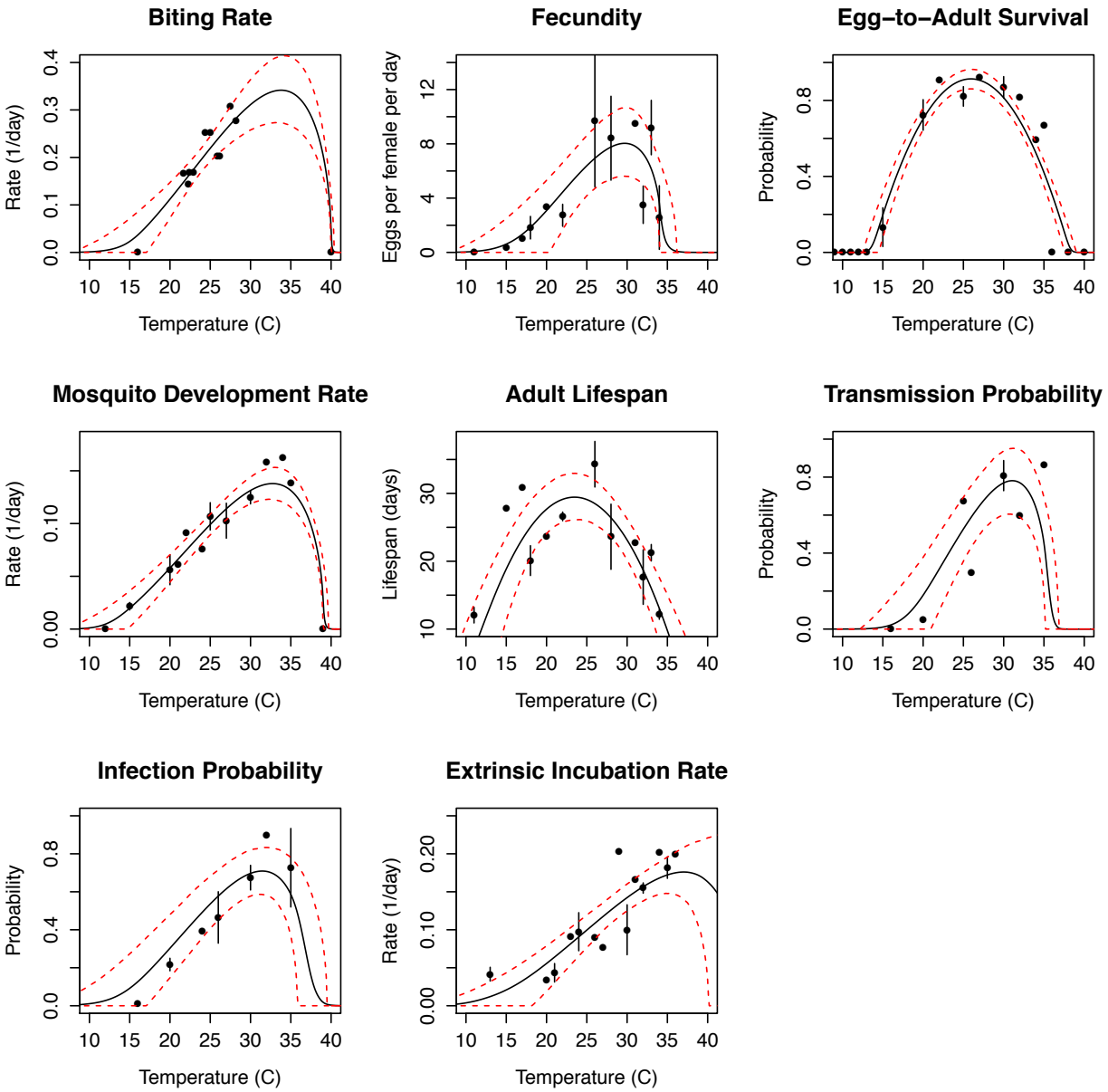
Biting Rate
Rate (1/day)
Temperature (C)
Fecundity
Eggs per female per day
Temperature (C)
Egg–to–Adult Survival
Probability
Temperature (C)
Mosquito Development Rate
Rate (1/day)
Temperature (C)
Adult Lifespan
Lifespan (days)
Temperature (C)
Transmission Probability
Probability
Temperature (C)
Infection Probability
Probability
Temperature (C)
Extrinsic Incubation Rate
Rate (1/day)
Temperature (C)

669 **Figure 2**

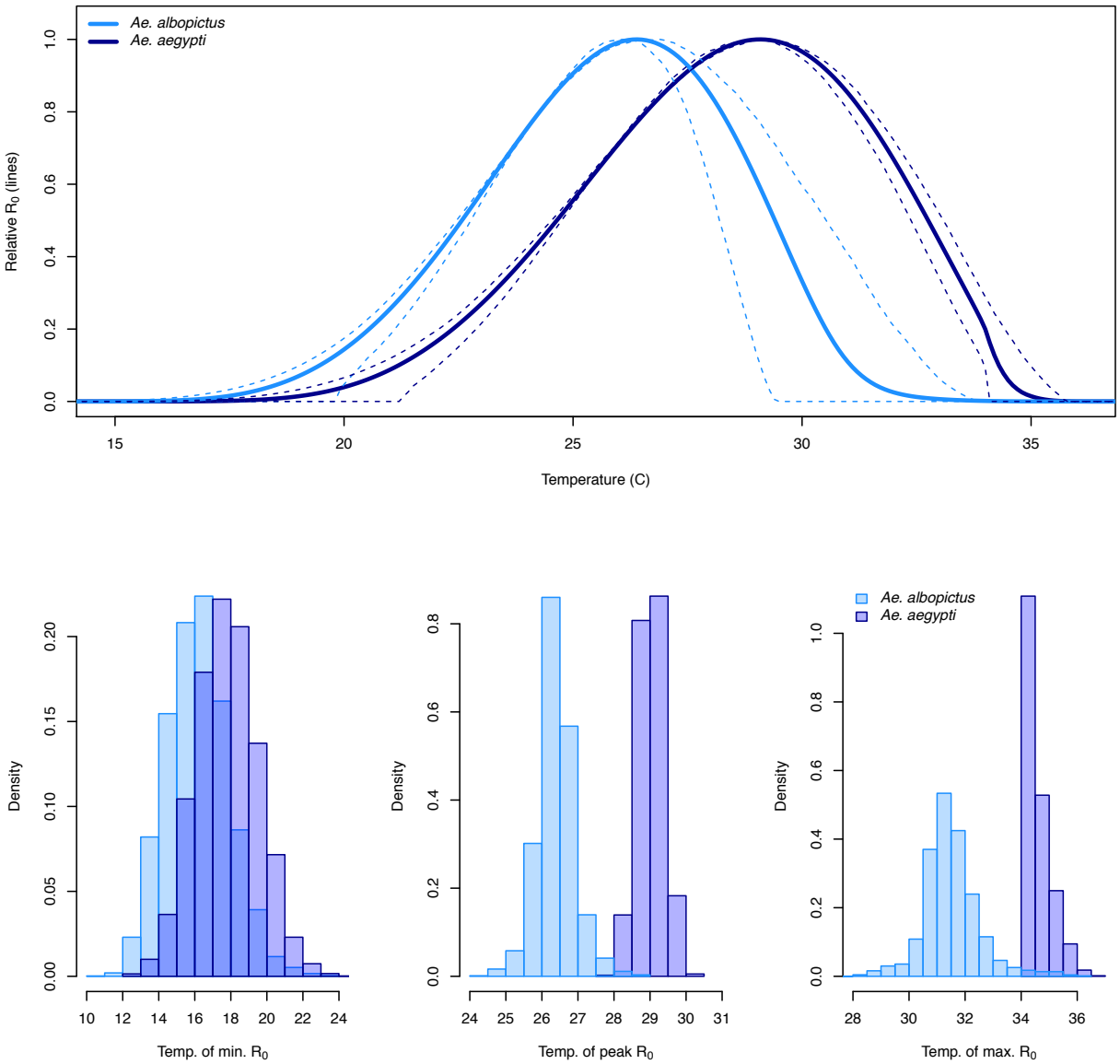

670
671

672 **Figure 3**

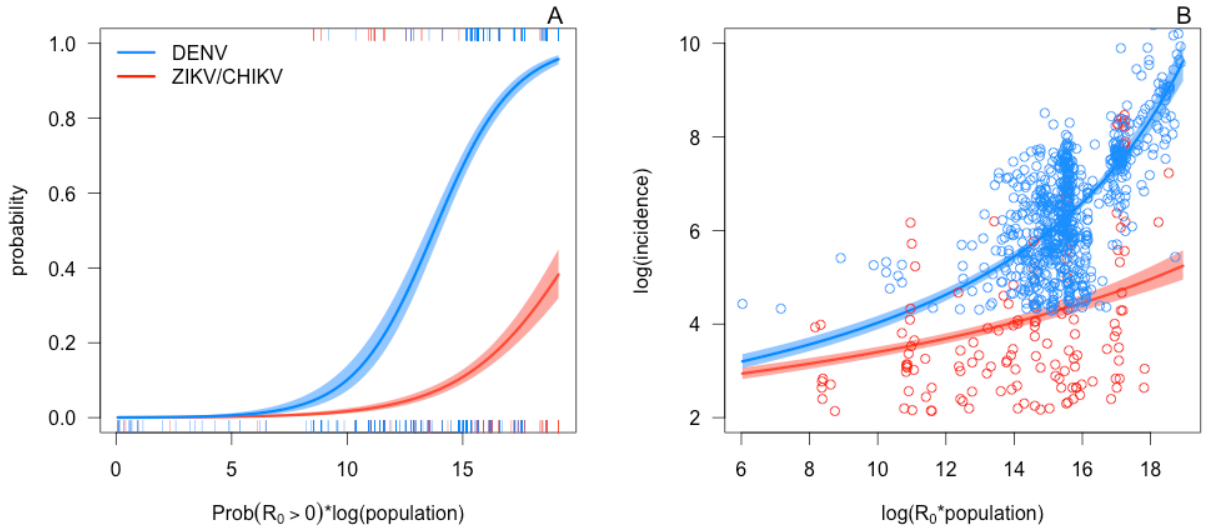

673
674

675 **Figure 4**

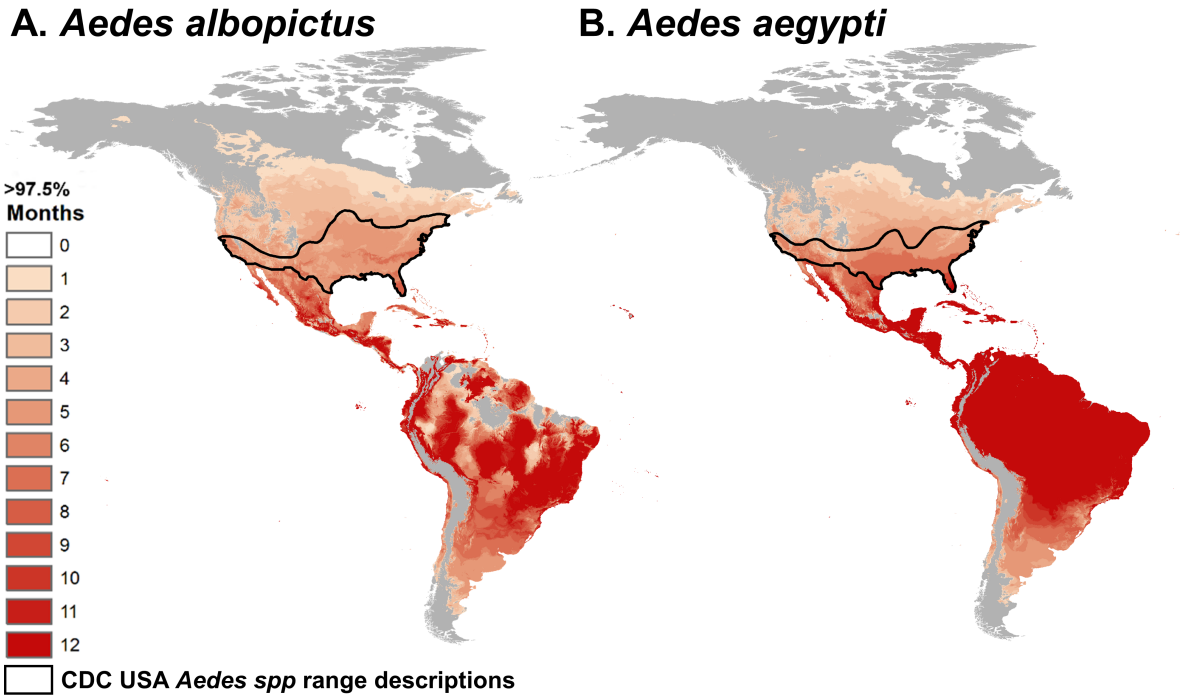

676
677